plants

MDPI

Article

In Dormant Red Rice Seeds, the Inhibition of Early Seedling Growth, but Not of Germination, Requires Extracellular ABA

Alberto Gianinetti

Council for Agricultural Research and Economics (CREA), Research Centre for Genomics and Bioinformatics, Via S. Protaso 302, 29017 Fiorenzuola d'Arda, PC, Italy; alberto.gianinetti@crea.gov.it

Abstract: The phytohormone abscisic acid (ABA) inhibits seed germination and seedling growth and is required for the inception of dormancy. Xanthoxal (also known as xanthoxin) is the first specific biosynthetic precursor of ABA. In this study, a modified method to produce xanthoxal is described. I tested the ability of either xanthoxal or ABA to reinstate dormancy in dormant red rice seeds whose dormancy was broken by fluridone (an inhibitor of the synthesis of carotenoids and, subsequently, ABA). Xanthoxal was shown to have a stronger inhibitory effect on germination than ABA when exogenously provided. Although this could indicate an additional effect of xanthoxal above that expected if xanthoxal were simply converted to ABA in the seed, alternative hypotheses cannot be excluded. One alternative is that exogenous xanthoxal may be trapped inside the cells to a greater extent than exogenous ABA, resulting in an intracellular level of ABA higher than that reached with a direct application of ABA. As a further alternative, exogenous xanthoxal may interfere with ABA action in the apoplast. In this study, following germination, early seedling growth was delayed only if ABA was applied. This suggests that inhibition of early seedling growth, but not of germination, requires extracellular ABA.

Keywords: seed dormancy; seedling growth; red rice; abscisic acid; fluridone; xanthoxal; xanthoxin

Citation: Gianinetti, A. In Dormant Red Rice Seeds, the Inhibition of Early Seedling Growth, but Not of Germination, Requires Extracellular ABA. *Plants* **2022**, *11*, 1023. https://doi.org/10.3390/plants11081023

Academic Editor: Anna Aksmann

Received: 9 March 2022
Accepted: 7 April 2022
Published: 9 April 2022

1. Introduction

Physiological dormancy is a state of the seed that, if not released, causes the seed not to germinate or to germinate slowly, even in conditions otherwise suitable for germination [1]. Dormancy is induced during seed maturation and can be relieved by the after-ripening of dry seeds or by the stratification of imbibed seeds [1].

"Red rice" is the common name of weedy rices, a heterogeneous group congeneric to crop rice and characterized by a red caryopsis [2]. These rices show various degrees of seed dormancy; as some accessions are fully dormant, red rice has been proposed as a model plant to elucidate the mechanisms of dormancy [3,4].

The plant hormones abscisic acid (ABA) and gibberellic acids (GAs) act antagonistically in multiple physiological processes, and their balance is critical to normal development and stress responses [5]. Specifically, ABA and GAs are antagonistically involved in seed dormancy and germination, with ABA predominating in dormant seeds and GAs in germinating seeds [1,6]. In particular, ABA is known to function in the process of post-germination growth arrest to protect nascent seedlings from an osmotic environment that turns increasingly stressful and may thus threaten seedling survival [7,8]. In such conditions, seedling growth ceases, and, for a short developmental window, the embryo can re-enter the developmental rest state [8]. This protects the seedling for some time, increasing its chances of encountering favourable conditions [6]. In this respect, the role of ABA in preventing early seedling growth is obvious.

ABA, indeed, has many roles in regulating plant growth, development, and the response to various environmental stresses [6]. Specifically, it shows multiple functions in several stages of seed development [6]. ABA synthesis (in the seed embryo) plays a critical

role in initiating dormancy; in fact, null mutations of ABA biosynthetic genes cause the breaking of seed dormancy in many species, including *Arabidopsis thaliana* [9,10], *Solanum lycopersicum* [11], and *Nicotiana plumbaginifolia* [12]. In barley, it has been suggested that the synthesis, catabolism, or removal of ABA, as well as sensitivity to ABA, concur to determine seed dormancy [13].

However, the role of abscisic acid (ABA) in maintaining seed dormancy is far from clear [14–16]. In this respect, it is worth pointing out that, even though exogenous ABA enters the embryo, it is not able to restore dormancy (more precisely, to prevent pericarp splitting) in seeds whose ABA synthesis is blocked unless very high non-physiological ABA concentrations are used [14]. Likewise, in many species, sensu stricto germination (testa rupture) of non-dormant seeds is not prevented by ABA [17]. In addition, the degree of dormancy does not always correlate with the dry seed ABA concentration [10,18], and, in wheat, after-ripening relieves seed dormancy without altering the dynamics of the ABA metabolism [19]. Moreover, the proteomic and transcriptomic profiles of dormant arabidopsis seeds differ from those of non-dormant seeds treated with ABA to block their germination and growth, indicating that the physiological state of dormant seeds differs from the state of seeds whose germination is blocked by ABA [20,21].

Fluridone, which blocks the synthesis of carotenoids by inhibiting phytoene desaturase [22], has been used in several studies to prevent ABA biosynthesis: this inhibitor causes the increased or hastened germination of imbibed dormant seeds of red rice [14], arabidopsis [23], barley [24], potato [25], and *Nicotiana plumbaginifolia* [26], among others. Interestingly, fluridone also increased germination in *Orobanche minor* [27] and annual ryegrass [15] without decreasing endogenous ABA levels, suggesting that this inhibitor was acting through a different mechanism. Indeed, an unidentified physiological modulator specific to dormancy and depleted by fluridone has been proposed to explain the inability of ABA to revert the promotion of germination by fluridone [14]. A reduction in the level of some carotenoid-derived molecule other than ABA has been specifically hypothesized to account for the incongruencies between the purportedly central role of ABA in maintaining seed dormancy and the findings mentioned above [28]. In this regard, it has been suggested that the immediate precursors of ABA might have intrinsic biological activity [29].

The enzyme 9-*cis*-epoxycarotenoid dioxygenase (NCED) cleaves C_{40} 9-*cis*-epoxycarotenoids (Figure 1A), specifically either 9-*cis*-violaxanthin or 9′-*cis*-neoxanthin (which is the 9-*cis*-epoxycarotenoid typically found in nature), to produce xanthoxal (whose structure is shown in Figure 1B). This reaction is the first committed step and the rate-limiting step in ABA biosynthesis [6,30], and it is necessary to maintain dormancy [10]. Hence, any carotenoid-derived molecule directly affecting dormancy must be produced by the cleavage of 9-*cis*-epoxycarotenoids to xanthoxal by NCED, or by a reaction occurring after it. In the seed, xanthoxal, the first C_{15} precursor of ABA, is translocated from the plastid to the cytosol, where it is converted to abscisic aldehyde and further to ABA [6]. The IUPAC name of xanthoxal ($C_{15}H_{22}O_3$) is (2Z,4E)-5-[(1S,4S,6R)-4-hydroxy-2,2,6-trimethyl-7-oxabicyclo [4.1.0]heptan-1-yl]-3-methylpenta-2,4-dienal (PubChem CID: 5282222), and its exact mass is 250.15689 Da.

As xanthoxal can enter the seed and then undergo all the conversion steps along the biosynthetic pathway to ABA [30,31], this molecule is the most interesting to test. It is worth noticing that though the common name of this molecule is xanthoxin, "xanthoxal" is recommended as the preferred name [32].

Mutants of *Arabidopsis thaliana* defective in ABA biosynthesis have been used to test possible specific effects of ABA precursors; the results show that although the biosynthetic precursors of ABA can trigger ABA responses in physiological assays, they have limited intrinsic bioactivity, and the physiological activity of ABA precursors derives predominantly from their conversion to ABA in planta [30]. That study used arabidopsis seeds whose dormancy had been fully broken [30], and when dormancy is completely removed (or is suppressed by a mutation of an ABA biosynthetic gene), sensitivity to ABA and to other factors repressing germination is drastically reduced [1,14,26,33,34]. Testing the capability of ABA precursors to maintain dormancy in seeds whose dormancy is relieved

by the simultaneous application of fluridone is a more specific assay to establish the effect of these molecules on seed dormancy, since high ABA sensitivity, typical of dormant seeds, is retained [14]. This test is the main purpose of the present research, and because prolonged incubation is required to test the effect on germination [14], I developed a modified procedure to produce enough xanthoxal to carry out the assay.

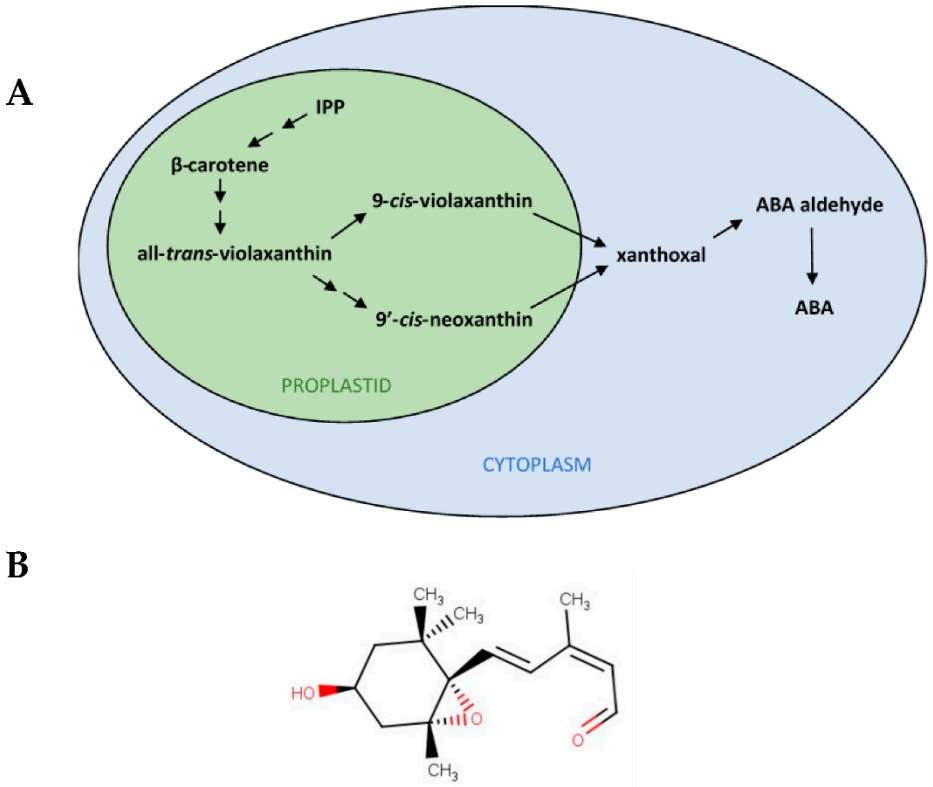

Figure 1. Xanthoxal features. (**A**) Scheme of the abscisic acid (ABA) biosynthesis pathway in plants. ABA synthesis proceeds from the carotenoid pathway, which starts from the precursor isopentenyl pyrophosphate (IPP), a C_5 (five carbon atoms molecule), and, through β-carotene, a C_{40}, produces epoxydic xanthophylls, such as all-*trans*-violaxanthin, still a C_{40}. By isomerization, 9′-*cis*-neoxanthin and 9-*cis*-violaxanthin are further obtained, which can be oxidatively cleaved by 9-*cis*-epoxycarotenoid dioxygenases (NCEDs) in the first specifically committed step of ABA synthesis, resulting in the production of xanthoxal, a C_{15}. Up to the C_{40} to C_{15} conversion, which is the rate-limiting step of ABA biosynthesis, the pathway takes place in the plastids (proplastids, in seeds). Thereafter, in the cytoplasm, ABA (still a C_{15}) is synthesized from xanthoxal through ABA aldehyde. Double arrows indicate multiple biosynthetic steps. (**B**) Chemical structure of *cis*,*trans*-xanthoxal (oxygen residues are evidenced in red), the biologically active form of xanthoxal.

If exogenous xanthoxal were capable of fully restoring dormancy and ABA were not, it could be inferred that xanthoxal or another ABA precursor produced through the bioconversion of xanthoxal in the seed has intrinsic bioactivity in addition to the physiological activity associated with the synthesis of ABA. Thus, in the present study, the capability of xanthoxal to restore dormancy by reverting the dormancy-breaking effect of fluridone is investigated. In order to accomplish this, a procedure is described that, by improving upon previous methods, allows the production of enough xanthoxal to carry out the test.

2. Results and Discussion

To obtain a sufficient amount of xanthoxal for the long germination test, several modifications were made to published methods (e.g., [31,35]) for both the extraction of

epoxydic xanthophylls (using environmentally acceptable solvents when possible; see [36]) and xanthoxal purification. Thus, although the principle of the method used here to produce xanthoxal (the oxidative cleavage of epoxydic xanthophylls with zinc permanganate) is well established [31], the usage of more recent routine purification procedures, such as solid-phase extraction (SPE), was introduced. As violaxanthin is more abundant than neoxanthin in green tissues (Supplementary Figure S1) [31,37], it was used for the routine production of *cis*,*trans*-xanthoxal. Once xanthoxal was produced, its identity was confirmed by chemical characterization. Thereafter, it was used for the germination test.

2.1. Xanthoxal Characterization

As assessed by High-Performance Liquid Chromatography (HPLC), a mixture of *cis*,*trans*-xanthoxal and *trans*,*trans*-xanthoxal (where the former is the bioactive form) was obtained by the photoisomerization of the *trans*,*trans*-xanthoxal produced from the oxidative cleavage of violaxanthin (Figure 2). The peak at 3.56 min (assumed to be *trans*,*trans*-xanthoxal) was almost the only isomer present prior to UV irradiation. After irradiation, another peak at 3.85 min was observed. Based on the literature, this latter was identified as the bioactive form *cis*,*trans*-xanthoxal [31]. Correspondingly, the oxidative cleavage of neoxanthin (without photoisomerization) produced this peak only, confirming that it corresponds to the *cis*,*trans* isomer of xanthoxal (not shown). This peak has a maximum at 284.5 nm and a (secondary) *cis* peak at 203 nm (c/h ratio 0.28), whereas *trans*,*trans*-xanthoxal has a maximum at 286.5 nm. The features of the UV−visible spectrum of a *cis* isomer are, indeed, a pronounced *cis* peak at wavelengths sharply shorter than λ_{max} and a very small displacement of λ_{max} itself toward shorter wavelengths [38]. Additional smaller peaks appeared at 2.90 and 3.14 min if irradiation was too intense and prolonged (as occurred for the sample shown in Figure 2). They are supposed to be *trans*,*cis*-xanthoxal and *cis*,*cis*-xanthoxal, respectively. As assessed by HPLC, the xanthoxal isomer mixture did not show a noticeable presence of contaminants (Supplementary Figure S2).

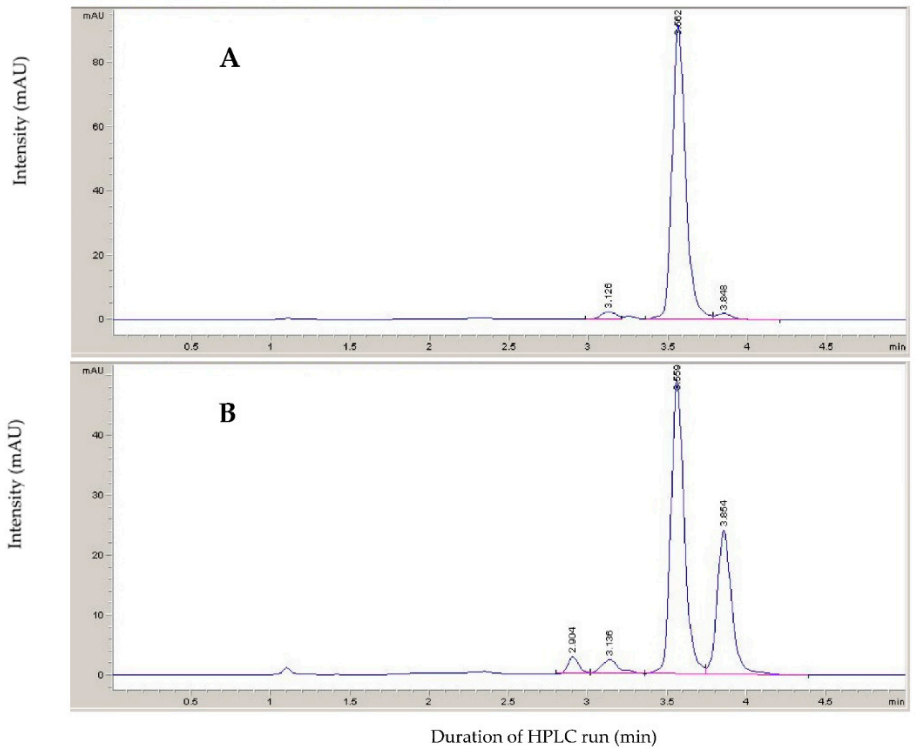

Figure 2. Chromatograms (at 285 nm; isocratic reversed-phase HPLC with 40% acetonitrile containing 0.02% triethylamine) of: (**A**) xanthoxal (dissolved in acetonitrile) produced by permanganate oxidation of violaxanthin; (**B**) the mixture of geometric isomers obtained after irradiation with a Wood lamp.

HPLC coupled with Electrospray Ionization Mass Spectrometry (LC-ESI-MS; Figure 3) confirmed that the obtained chemical had the molecular weight expected for xanthoxal (250.16 Da, to which a proton is added during ESI^+ to form a quasi-molecular ion denoted $[M + H]^+$). The oxygen atoms act as proton attractors, with different outcomes: if the proton hydrogenates the hydroxy group, water is then easily released, and a secondary carbocation is produced (m/z 233.16) that can undergo a resonance effect (not shown); if the epoxide is attacked, it opens easily because of its strong steric strain, and thereby a hydroxy group and a tertiary carbocation at the two involved carbon atoms form, with two possible isomers. The terminal carbonyl oxygen is less susceptible to proton attack because of the stability of the conjugated double bonds in the side chain, which are disrupted by the formation of a carbocation. Thus, the molecular peak (m/z 251.17) is expected to correspond to two isomeric tertiary carbocations (more stable than secondary carbocations), although a resonance effect with secondary carbocations is possible (not shown). The putative chemical structure of the main fragments obtained from tandem mass spectrometry (MS/MS, wherein the molecular ion is selected and then split into smaller fragment ions by collision-induced dissociation) is proposed (Supplementary Figures S3 and S4) to show that they are closely compatible with what may be expected from the ESI^+ fragmentation of the xanthoxal molecule (whose ESI^+ fragmentation pattern was not available in public databases). Thus, based on the absorbance and mass spectral features, and given it was obtained through the oxidative cleavage of violaxanthin (a process that is known to produce xanthoxal [31]), the isomer generated by photoisomerization was identified as *cis*,*trans*-xanthoxal with high confidence.

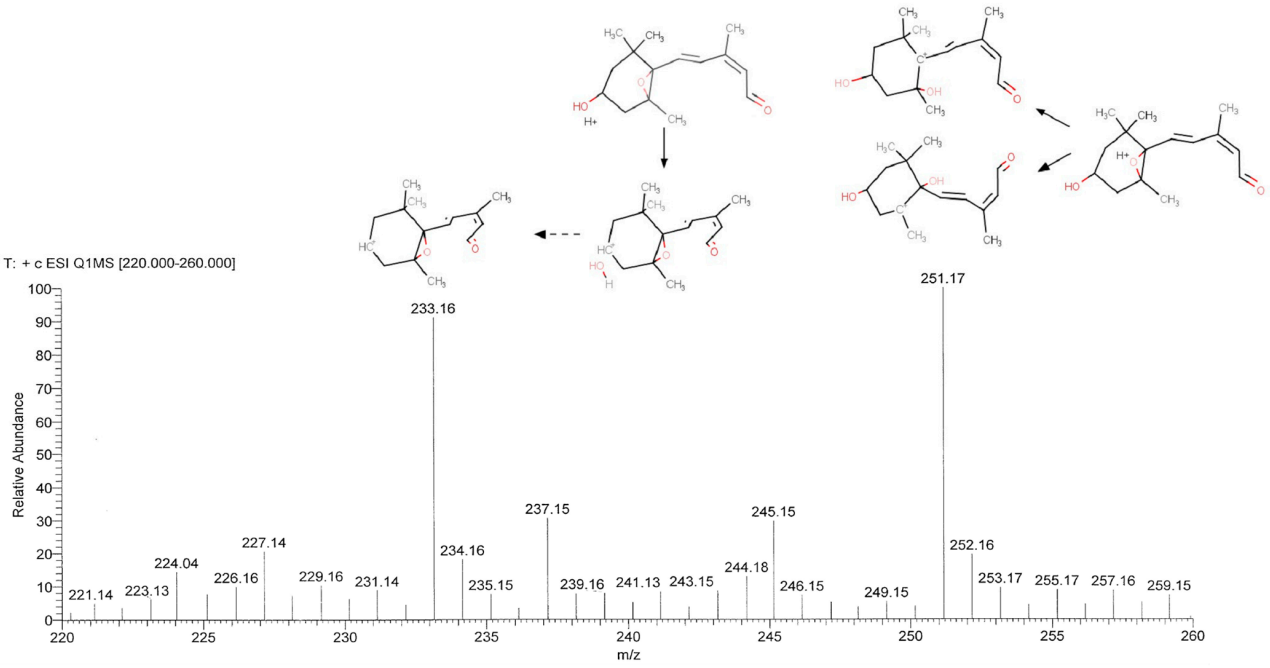

Figure 3. LC-ESI-MS analysis of the (unfragmented) molecule identified as xanthoxal. Two major peaks were observed, with m/z values of 251.17 and 233.16, corresponding to the protonated molecule and its dehydrated form, respectively. The putative structures (based on the *cis*,*trans*-xanthoxal isomer) above each main peak represent the proposed identification of the molecule.

2.2. Germination Test

Xanthoxal was assayed for its ability to maintain seed dormancy in red rice dormant seeds whose physiological dormancy was simultaneously removed by fluridone (Figure 4A). Both 10 µM (±)-ABA (expected to correspond to 5 µM (+)-ABA [39]) and 5 µM *cis*,*trans*-xanthoxal (applied as part of a mixture of *cis*,*trans*-xanthoxal and *trans*,*trans*-xanthoxal) were able to reduce the percentage of seeds that achieved early seedling growth at similar levels (Figure 4B), confirming that both were biologically active.

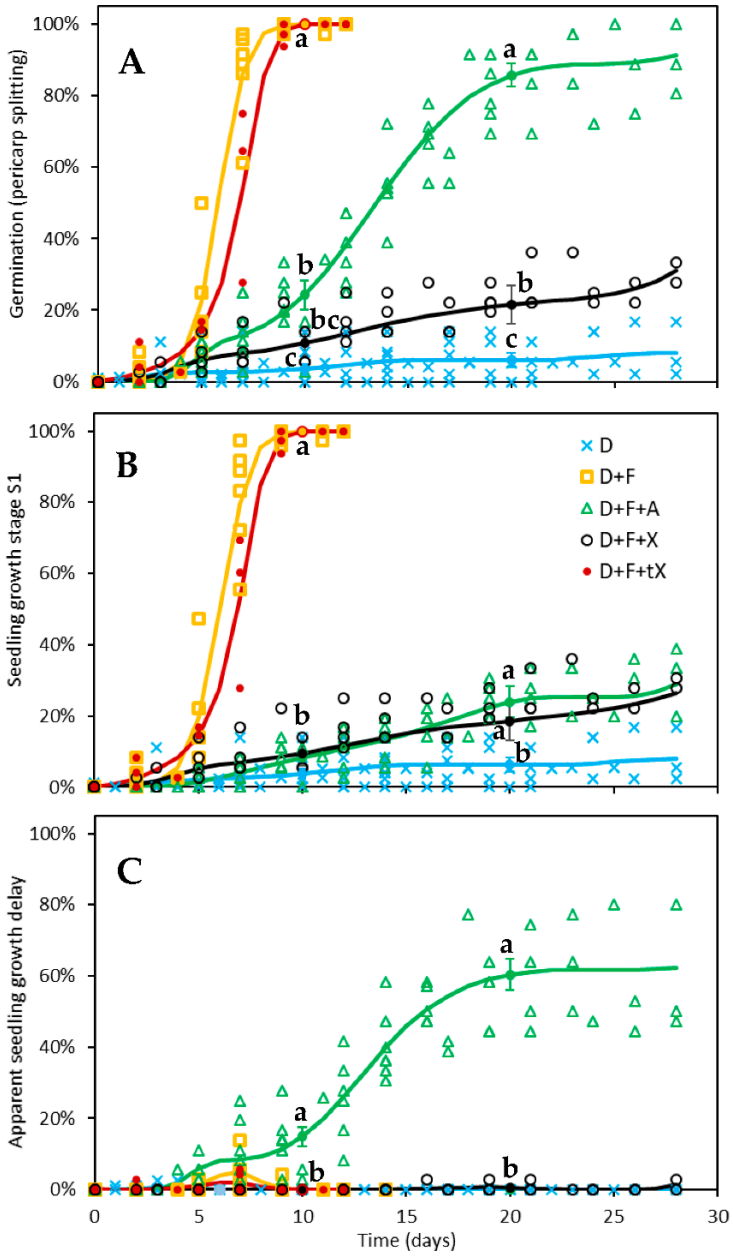

Figure 4. Germination and early seedling growth time-courses of dormant red rice seeds incubated in: 20 mM BTCA pH 4.4 (D, blue crosses) treated with 10 µM fluridone (D + F, yellow squares) plus either 10 µM racemic (±)-ABA (D + F + A, green triangles) or 5 µM *cis*-xanthoxal (D + F + X, black circles) or 5 µM *trans*-xanthoxal (D + F + tX, red-filled circles). Every treatment was replicated across three to six independent experimental runs, whose individual datapoints are shown in each plot. A datapoint typically represents the mean of 2–6 (typically 3) replications (12 seeds each). The number of treatment repeats (trp) and of seeds (n) tested for each treatment were as follows: D trp = 6 n = 276, D + F trp = 6 n = 204, D + F + A trp = 6 n = 251, D + F + X trp = 4 n = 144, D + F + tX trp = 3 n = 120. (**A**) Germination percentage (assessed as pericarp splitting). (**B**) Percentage of seeds attaining first growth stage (S1, i.e., rootlet or coleoptile $\geq$ 1 mm). (**C**) Difference between observed percentages of growth stage S1 and germination, indicative of a delay of seedling growth once germination was attained. Lines represent the time-course trends based on GzLMM estimations. Statistical differences among treatments were tested at 10 and 20 days ($p \leq 0.05$ within each date; Holm-Sidak test): at each timepoint, treatments labelled with the same letter are not significantly different from each other (only one letter is shown for overlapping responses belonging to the same significance group). Error bars indicate standard errors.

ABA prevents seedling growth; however, at physiological concentrations, it cannot re-establish seed dormancy; that is, it cannot persistently block germination [14]. The splitting of the seed-covering layers (i.e., the caryopsis coat, in the case of rice kernels) above the embryo is the conventional marker of germination and, therefore, of dormancy breaking [17]. However, some embryo growth (expansion) is necessary even to accomplish the rupture of the covering layers [17], and ABA can therefore delay pericarp splitting, but it cannot prevent it [14]. Exogenous ABA is more effective at a lower pH level [14] due to the ion-trap mechanism that causes the phytohormone to accumulate in the cellular symplast [14,40]. This might occur because of free diffusion across the cell membrane, but the key role of transporters has increasingly been acknowledged [41,42]. Specifically, some transporters of the ABC (ATP-Binding Cassette) family have been shown to suppress arabidopsis seed germination by importing ABA from the endosperm into the embryo [43]. Although the mechanism of action of the ABA transporters is not yet clear, they favour the passage of ABA through the cell membrane, and, therefore, they should generally facilitate the ion-trap mechanism, since the effect of pH on symplastic-apoplastic ABA equilibration is indisputable [41].

Xanthoxal, however, was able to largely prevent pericarp splitting (i.e., the rupture of the seed testa, or, more precisely, of the caryopsis coat; Figure 4A). Even though *cis*,*trans*-xanthoxal was only partially able to restore dormancy (or, more properly, to restrain germination), it was more effective than ABA (Figure 4A). Since xanthoxal is not expected to be physiologically active in the apoplast, its capability to inhibit germination also confirms that xanthoxal can enter the seed and be converted to ABA [30,31,44]. Given that ABA moves into the cells through specific transporters [42,45] and the xanthoxal molecule is similar to ABA, it may be assumed that xanthoxal can be carried inside the cell by the same transporters that carry ABA. However, xanthoxal conformation is quite different from that of ABA [46]; thus, such transporters must not be very specific.

The greater effectiveness of xanthoxal with respect to ABA was, indeed, found by Taylor and Burden [31] and Kepka et al. [30] for the inhibition of germination in non-dormant seeds of *Lepidium sativum* and *Arabidopsis thaliana abi1-1* mutant, respectively. It is worth noticing that, on the one hand, the stronger effect of xanthoxal observed in the present study cannot be due to the concomitant presence of *trans*,*trans*-xanthoxal in the mixture of *cis*,*trans*-xanthoxal and *trans*,*trans*-xanthoxal, since *trans*,*trans*-xanthoxal (non-photoisomerized xanthoxal from violaxanthin) is not effective (Figure 4A; a very small effect was seen at around 7 d, but this was most probably due to ~5% *cis*,*trans*-xanthoxal that was present, perhaps because light cannot be entirely avoided during xanthoxal preparation). In fact, *trans*,*trans*-xanthoxal is not converted to ABA in planta [47]. On the other hand, it is possible that the unnatural (-)-ABA enantiomer has some biological effect [39]; if true, this would make the result obtained with *cis*,*trans*-xanthoxal even more compelling. Thus, the greater effectiveness of xanthoxal over ABA was the most apparent finding of the germination tests.

A second noticeable finding was that, once germination occurred, seedling growth immediately followed if dormant seeds treated with fluridone were also given xanthoxal, but seedling growth was delayed if ABA was applied instead (Figure 4B,C). Thus, the stronger inhibitory effect on germination of xanthoxal compared to ABA seems to confirm a direct effect of xanthoxal on the maintenance of seed dormancy, but the lack of inhibition of seedling growth by xanthoxal revealed unexpected complexity in the response.

The inhibition of seedling growth by exogenous ABA was accompanied by a secondary effect: during early growth, the embryo collar (see [48] for a description) showed some browning, apparently due to a mild superficial necrosis, and the development of rhizoids was largely curbed (Supplementary Figure S5). This could be interpreted as a sort of physiological disequilibrium, but it is hard to quantify, even more so because rhizoids are ephemeral structures that atrophy in a few days regardless. Browning was much rarer when dormant seeds induced to germinate by fluridone were treated with xanthoxal rather than ABA: as said, once these seeds attained pericarp splitting, they continued to grow into

seedlings without delay; these seeds were able to develop, albeit with wide variability, a thick tuft of rhizoids, as commonly happens when only fluridone, and not ABA, is applied (Supplementary Figure S5). This seems to suggest that the application of ABA might have brought extracellular (apoplastic) ABA to a higher level than that occurring with a normal, physiological equilibration between symplastic and apoplastic ABA. Exogenous xanthoxal did not provoke this effect, probably because it is not biologically active in the apoplast, and the ABA produced in the symplast from exogenously provided xanthoxal necessarily underwent a more physiological equilibration of its apoplastic level according to the ion-trap mechanism [40]. In accordance, no delay in seedling growth was observed for the few seeds that germinated in the untreated control (also at pH 4.4).

Although *cis*,*trans*-xanthoxal appears to be a better molecular effector of seed dormancy than ABA, it might be argued that xanthoxal is more effective at retrieving seed dormancy (more precisely, inhibiting germination) than ABA because of differences in the trans-membrane compartmentation when either one or the other of these molecules is provided exogenously. In fact, symplastic ABA is in equilibrium with apoplastic ABA, as ABA can move in and out of the cells, but this equilibrium depends on the ion-trap mechanism (since only the non-ionized form can cross the membrane [40]), and this kind of equilibrium should, therefore, be substantially different for xanthoxal, which does not have an ionic form. Specifically, since xanthoxal does not ionize in the apoplast, its uptake into the symplast ought to increase with respect to ABA. In the long run, however, if the transporters that import xanthoxal into the cell, possibly the very same that import ABA, were also responsible for exporting these molecules out of the cell, xanthoxal would not be trapped in the cells. In such case, in fact, xanthoxal would be able to move out of the cell to the same extent as it moved in, apart from the xanthoxal that is metabolized to ABA inside the cell. Xanthoxal, however, is not known to be usually exported outside of seed cells. Therefore, different transporters should be responsible for importing and exporting ABA (this is, indeed, a known fact [6,42]), and only the transporters for the import of ABA into the cell should also be able to transport xanthoxal, whereas those for the export of ABA from the cell should not. If this were true, exogenous xanthoxal would indeed be trapped inside the cells much more effectively than exogenous ABA.

In accordance with the proposed hypothesis of the important role of transporters in determining the cellular concentration, and thus the effect, of these kinds of molecules, an ATP-Binding Cassette (ABC) transporter, MtABCG20, was shown to function as an ABA exporter in germinating seeds of *Medicago truncatula*, and the germination of the loss-of-function mutant, *mtabcg20*, was more sensitive to ABA due to the impairment of ABA export [49]. Of course, this is possible because, even though there are many ABA transporters, each plays a specific role under a given condition and in a specific tissue, so that they are not completely redundant [45].

As said, once xanthoxal is transformed into ABA in the cytoplasm, symplastic-apoplastic ABA equilibration occurs [40,41]. Xanthoxal is indeed rapidly converted to ABA in planta [47], as its conversion is catalysed by enzymes that are constitutively expressed in plant tissues [50] (p. 225). Thus, at equilibrium, ABA derived from (the cellular conversion of) exogenous xanthoxal is expected to block seedling growth at the same level as exogenous ABA, given that the same amount of biologically active (S)-ABA would ultimately be provided, in the two treatments, to the symplast as well to the apoplast. A similar level of inhibition of seedling growth was indeed observed for the two conditions; however, in xanthoxal-treated seeds, seedling growth was prevented only if pericarp splitting (germination) was prevented too (Figure 4A,B). In ABA-treated seeds, on the other hand, seedling growth was delayed following germination (Figure 4C). Some mechanism, therefore, hampers a comparable symplastic-apoplastic ABA distribution across the two treatments.

Thus, the stronger inhibition of germination (assessed using pericarp splitting as a visual marker) by exogenous xanthoxal seems to suggest two possibilities. Either the application of xanthoxal causes a higher ABA concentration inside the cells than if ABA

itself is applied (that is, the equilibrium between symplastic and apoplastic ABA is not reached because, for example, ABA is continuously produced inside the cell faster than it is exported to the apoplast) or, instead, xanthoxal has an effect per se (as suggested long ago [51]), that is, it is recognized by some intracellular receptor as a biologically active molecule. On the basis of the ion-trap mechanism, however, the former hypothesis seems doubtful, as the equilibration between intracellular and extracellular ABA ought not to be a slower process than the ABA biosynthesis from xanthoxal. Nevertheless, this might occur if the equilibrium between symplastic and apoplastic ABA is not reached because some limiting mechanism operates to restrain ABA import but not xanthoxal import when intracellular ABA concentration reaches some threshold. On the one hand, this additional hypothesis is more consistent with the above-mentioned observation that the application of ABA might bring apoplastic ABA to a higher level than that occurring with a physiological equilibration between symplastic and apoplastic ABA. On the other hand, the existence of such a mechanism has never been demonstrated. In addition, this hypothesis also requires that the ABA produced from xanthoxal in the symplast is, in turn, prevented from reaching the same apoplastic level as when ABA is provided. Although this could be explained by a quick intracellular catabolism of any ABA excess, the present findings reveal that something is missing in our present understanding of the regulation of ABA response/transport/catabolism. As for the latter hypothesis (namely, that xanthoxal has an effect per se), since the biological effects of xanthoxal are very close to those of ABA, and the xanthoxal molecule is similar to ABA, one might suppose that xanthoxal acts on ABA receptors, as noticed above for ABA transporters. However, conformational differences between xanthoxal and ABA [46] make this assumption even more speculative for receptors than for transporters. In fact, xanthoxal is expected to have a poor affinity for PYL receptors, given that the carboxylic moiety has a role in forming a stable complex with the receptor to trigger a signal [46]. Dedicated intracellular xanthoxal receptors, on the other hand, are expected to cause a complete reversal of the effect of fluridone, with full restoration of dormancy in seeds treated with xanthoxal, given that they were provided with a relatively high xanthoxal amount. Such a complete reversal, however, did not occur. Thus, both hypotheses seem to fall short of providing a satisfactory explanation for the observed results, at least based on the present knowledge. Yet, our knowledge of PYR/PYL ABA receptors is still limited, and relevant differences in their properties have been observed among different species [52].

In any case, the diverging effects of applied xanthoxal on germination and seedling growth indicate that different receptors are involved in the control of germination (pericarp splitting) and early seedling growth (rootlet or coleoptile $\geq$ 1 mm). An easy explanation for the observed separation of the two effects (namely, strong inhibition of germination but no inhibition of seedling growth following germination) is that hormone receptors negatively controlling germination and seedling growth are located in the symplast and the apoplast, respectively. ABA, indeed, can be perceived at both intracellular and extracellular sites [53]. A divergence in the response to exogenous ABA between radicle emergence and seedling growth has also been observed for the suppression of ABA inhibition by low concentrations of sugars in arabidopsis [54]. In that case too, either an alteration of ABA availability at one site of ABA perception or of a specific signalling pathway was suggested to be responsible for the two independent responses [54]. In the present case, as xanthoxal is physiologically converted to ABA inside the cells, a different localization of ABA receptors affecting radicle emergence and seedling growth appears to be the most obvious explanation for the divergent responses observed at these two stages when either xanthoxal or ABA were exogenously provided.

As a further alternative hypothesis to explain why exogenous xanthoxal inhibited pericarp splitting but not seedling growth, which immediately followed whenever pericarp split occurred, whereas exogenous ABA delayed seedling growth after pericarp splitting, it might be supposed that ABA effectiveness was lower at the site of growth control (possibly the apoplast) in xanthoxal-treated seeds than in ABA-treated seeds. Assuming

that xanthoxal is quickly converted to ABA in the cytoplasm and that a normal equilibrium between symplastic and apoplastic ABA would then be promptly achieved, it could be hypothesized that exogenous xanthoxal would negatively interfere with ABA signalling in the apoplast (where, physiologically, there should not be xanthoxal). Maybe they compete for the same receptors, but xanthoxal does not elicit a response. Even in this case, the hypothesis that hormone receptors repressing germination and seedling growth are located in the symplast and apoplast, respectively, would provide a simple explanation for the diverging effects of exogenous xanthoxal vs. exogenous ABA on germination and seedling growth. So, at present, there are several possible explanations for the greater efficacy of xanthoxal over ABA, but whatever the correct explanation is, an apoplastic localization of ABA receptors for the inhibition of seedling growth is highly consistent with the present findings.

Further research involving a more detailed analysis of xanthoxal and ABA levels in the apoplast and symplast is necessary to disentangle this matter and answer all the questions raised by the present study.

3. Materials and Methods

3.1. Chemicals

Stock solutions were prepared by dissolving fluridone (Duchefa, Haarlem, The Netherlands) and racemic (±)-ABA (Sigma, St Louis, MO, USA) in dimethylsulphoxide (DMSO; Sigma, St Louis, MO, USA) to a concentration of 0.1 M. Xanthoxal (a mixture of geometric isomers produced as detailed below) was dissolved in DMSO to a concentration of 0.1 M (total xanthoxal). If the DMSO volume required to prepare a new xanthoxal stock was <200 µL, the stock volume was brought to 200 µL with a 20% (weight for volume of water) aqueous solution of polyethylene glycol (PEG) 6000 (BDH, Poole, UK). Pre-dilution to such minimum volume was necessary to wash all the xanthoxal off the walls of the vial. These stock solutions were stored at +5 °C, wrapped with aluminium foil; pre-diluted xanthoxal stock was prepared just before the experimental run (with a freshly dissolved PEG solution). The seed incubation solution was buffered to pH 4.4 with 20 mM 1,2,3,4-butanetetracarboxylic acid (BTCA; Aldrich, Steinheim, Germany) [14].

3.2. Xanthoxal Production

3.2.1. Extraction of Xanthophylls

Freshly collected maize leaves (about 300 g) were immediately immersed in 50:50 ethanol/ethyl acetate (600 mL) while protecting them from direct sunlight. Ten grams of sodium bicarbonate was gradually added together with the leaves into an amber bottle. A needle through the cap prevented pressure build-up. After overnight extraction, the liquid was percolated, and the leaves were extracted again with ethyl acetate overnight. This was repeated for a third extraction. The extracts were progressively combined while the volume was reduced by means of a vacuum rotary evaporator (Heidolph Instrument, Kelheim, Germany) at ≤30 °C. When evaporation slowed down, 50 g K_2HPO_4 was added. Whereas ethanol, which is a mildly chaotropic agent, was used in the first extraction to obtain a single phase from the organic (ethyl acetate) and the aqueous phases, K_2HPO_4, which is a strongly kosmotropic salt, was subsequently added to again separate (salting out) the two phases [55]. The volume was further reduced, and the liquid was discharged when it appeared to be dark yellow (in leaf extracts, the aqueous phase is yellow because of flavones [56]) as the chlorophylls sedimented on the rotating flask wall (indicating that the liquid was mostly water, since chlorophylls remain fully soluble when there is ≥15% ethanol).

3.2.2. Liquid-Liquid Partition of Xanthophylls

The sediment was re-suspended in 200 mL 90:10 hexane/ethyl acetate and transferred to a separatory funnel. Then, 200 mL 80:20 methanol/water was added, the mixture was thoroughly mixed, and two (green) layers were left to separate. Epoxydic xanthophylls

partitioned to the lower methanolic phase, and the upper one was therefore discharged. The methanolic phase was washed two more times with 200 mL 90:10 hexane/ethyl acetate to remove most chlorophylls. A small excess K_2HPO_4 (about 1 g) was then added to the methanolic phase. A small volume of aqueous phase (which is yellow because of flavones [56]) and the undissolved salt were discharged. A small amount of sodium sulphate was added, and the liquid was slowly percolated through filter paper. The organic phase was transferred to a flask, and 20 mL ethanol and a small excess of K_2HPO_4 were added. The volume was reduced with a rotary evaporator, but complete drying was avoided. Then, 100 mL 80:20 hexane/ethyl acetate was added, and part of the sediment was re-dissolved. The liquid was transferred to a new flask, a small amount of sodium sulphate was added, and the organic phase was slowly percolated through filter paper. The extract was stored under N_2. The analytical determination of carotenoids was performed with normal-phase HPLC (see Section 3.3.1. HPLC Analyses).

3.2.3. Purification of Violaxanthin and Neoxanthin with Solid-Phase Extraction

To further remove salts, chlorophylls, and most lutein, solid-phase extraction (SPE) was carried out with a silica column (60 mL, 10 g silica-Discovery®, Supelco; under suction). The column was conditioned (and deacidified) with 20 mL 80:20 hexane/ethyl acetate containing 1% triethylamine (TEA). After loading the sample (about 100 mL, in 80:20 hexane/ethyl acetate), violaxanthin was eluted with 100 mL di 50:50 hexane/ethyl acetate containing 0.05% TEA. Some chlorophylls eluted first and were discharged. Neoxanthin was eluted with 70 mL ethyl acetate. Normal-phase HPLC (see Section 3.3.1. HPLC Analyses) was used to check the purity of the two epoxydic xanthophylls. If they were satisfactorily pure, they were dried with a rotary evaporator, re-suspended in 1–2 mL acetone, collected in a small vial, and dried under N_2 flow. The weight of each xanthophyll was calculated by difference, and the two vials were stored at +5 °C.

To remove lutein from the violaxanthin fraction, SPE with a 2 g C18 column (Discovery®, Supelco; under suction) was performed. The column was pre-treated with 4 mL acetone, deacidified with 8 mL 25 mM K_2HPO_4, washed (de-salted) with 10 mL water, and conditioned with 7 mL 5:2 acetone/water containing 0.2% TEA. The dried violaxanthin fraction was dissolved in 7 mL 5:2 acetone/water containing 0.2% TEA, and it was then loaded. The column was then washed with 14 mL 5:2 acetone/water containing 0.05% TEA. Violaxanthin was eluted with 7 mL 6:1 acetone/water. The fraction was dried with a rotary evaporator, re-suspended in 1–2 mL 80:20 hexane/ethyl acetate (acetone could dissolve some residual salt), and transferred to a glass vial. Purity was checked in normal-phase HPLC (see Section 3.3.1. HPLC Analyses). If satisfactory, the sample was dried and stored as described above.

If some chlorophyll contamination persisted in a xanthophyll fraction, further SPE was carried out with a 1 g silica column (Discovery®, Supelco; under suction) as follows. The dried xanthophyll sample was dissolved in 2 mL acetonitrile (ACN) containing 0.25% TEA. The column was pre-treated with 2 mL ACN, deacidified with 5 mL 20% ACN in water containing 0.2% TEA and 2% K_2HPO_4 (w/v), and then conditioned with 10 mL ACN. After loading the sample, the epoxydic xanthophyll was eluted with ACN. Purity was then checked in reversed-phase HPLC with ACN/water (see Section 3.3.1. HPLC Analyses). If satisfactory, the epoxydic xanthophyll fraction was partitioned three times to diethyl ether by adding a small volume of diethyl ether, mixing, and then adding three times as much water as the volume of the ACN (i.e., the original volume of the eluted fraction). It was finally dried and stored in a small vial as described above. For long storage, epoxydic xanthophylls were kept at −20 °C.

3.2.4. Production of Xanthoxal by Oxidation of Epoxydic Xanthophylls

Xanthoxal was produced by the oxidative cleavage of epoxydic xanthophylls with zinc permanganate [31]. To minimize the oxidative degradation of xanthoxal once formed, equimolar concentrations of xanthophyll and permanganate were used (assuming that a

xanthophyll molecule should be cut once, and a molecule of permanganate is required to cleave one double bond). As part of the epoxydic xanthophyll remained un-cleaved after the oxidation, additional cycles of xanthophyll separation/oxidative cleavage were carried out. In the case of violaxanthin, which is symmetric and can therefore produce two xanthoxal molecules, C_{25}-epoxy-apocarotenal (the molecule that is produced together with xanthoxal with a single oxidative cut) and other epoxy-apocarotenals were combined with un-cleaved violaxanthin and subjected to oxidative cleavage again. Two to four oxidative cleavages were usually necessary to cleave all the violaxanthin and the allenic-apocarotenals (chiefly, C_{25}-epoxy-apocarotenal) derived from it. Two oxidative cleavages were often enough for neoxanthin, as the C_{25}-allenic-apocarotenal and other allenic-apocarotenals cannot produce xanthoxal.

For the first oxidative cleavage (100 µmoles of each compound), 60 mg epoxydic xanthophyll (from multiple collections) was dissolved in 14 mL acetone in a 50 mL Falcon tube, 18.3 mg zinc acetate was dissolved in 1 mL water, and 15.8 mg $KMnO_4$ was dissolved in 1 mL water. To the acetonic xanthophyll solution, 4.7 mL 0.2 M BTCA buffer pH 6 buffer, the permanganate solution (1 mL), and 300 µL of the zinc acetate solution were added. If smaller amounts of epoxydic xanthophyll were available (particularly in the case of neoxanthin), the reagent volumes were scaled down proportionally (in a 15 mL Falcon tube, if epoxydic xanthophyll was <20 mg). The mix was intermittently mixed by vortexing at slow speed for 10 min. One volume of diethyl ether was added to extract xanthoxal, apocarotenals, and residual xanthophyll. After thoroughly mixing, the mix was centrifuged for 5 min at 1000× *g*. The yellowish organic (upper) phase was transferred to a 250 mL round-bottom flask. The aqueous (lower) phase was re-extracted with diethyl ether by mixing and centrifuging as above. This second organic extract was united with the first one, and the sample was slowly dried with a rotary evaporator.

To separate xanthoxal, the dry sample was re-suspended in 4 mL ACN, 6 mL water was added, and SPE was performed with a 2 g C18 column (Discovery®, Supelco; under suction). The column was pre-treated with 4 mL ACN, conditioned and deacidified with 10 mL 40% ACN containing 0.5% K_2HPO_4. The xanthoxal fraction was collected from sample loading (in 40% ACN) up to elution with 10 mL 40% ACN. Residual xanthophyll and C_{25}-epoxy-apocarotenal were eluted with 6 mL ethyl acetate and dried with a rotary evaporator.

Second, third, and even fourth oxidative cleavages were performed on the residual xanthophylls with the same procedure and doses of permanganate and zinc acetate as above (assuming that all the cleaved violaxanthin produced C_{25}-epoxy-apocarotenal). When all the useful cleavages had been practically achieved (as judged from the colour intensity of the residual xanthophyll fraction or by normal-phase HPLC; see Section 3.3.1. HPLC Analyses), the xanthoxal fractions obtained from the various oxidation steps were combined. The overall yield of xanthoxal was quite low, roughly 10%, since there are several double bonds at which oxidative cleavage can occur, but only two in violaxanthin and one in neoxanthin are conducive to xanthoxal production, provided that double bonds internal to the xanthoxal residue are not cleaved as well.

3.2.5. Purification of Xanthoxal with Reversed-Phase SPE

To concentrate xanthoxal and remove most of the unwanted xanthophyll fragments as well as colloidal manganese oxides, three volumes of water was added to the xanthoxal solution (in 40% ACN), and SPE with a 2 g C18 column (Discovery®, Supelco) was carried out (under suction). The column was pre-treated with 4 mL ACN, conditioned and deacidified with 10 mL 10% ACN containing 0.5% K_2HPO_4. After loading the sample (in 10% ACN), the column was washed with 10 mL 10% ACN containing 0.5% K_2HPO_4 (to remove any residual manganese and zinc cations) and then with 20 mL 25% ACN. Xanthoxal was eluted with 10 mL 40% ACN. Different fractions were collected (typically three, of 2, 6, and 2 mL, respectively) and analysed with reversed-phase HPLC with 40% ACN isocratic flow (see Section 3.3.1. HPLC Analyses). Fractions containing xanthoxal were

combined. The *trans*,*trans*-xanthoxal could still display a yellowish colour due to traces of polar contaminants, presumably long carotene dialdehydes derived from violaxanthin.

The xanthoxal sample (in 40% ACN) was diluted with 1/3 of water (*v*/*v*) to 30% ACN, and then partitioned to diethyl ether three times. The latter was then dried almost completely (in a glass vial) under N_2 flow.

3.2.6. Photoisomerization

Oxidative cleavage of neoxanthin (which is naturally present as 9′-*cis*-neoxanthin) directly produces the bioactive *cis*,*trans*-xanthoxal form; thus, that neoxanthin is the preferred natural molecule for producing bioactive xanthoxal. Nevertheless, violaxanthin is much more abundant than neoxanthin in green tissues; it is therefore a better source for producing *cis*,*trans*-xanthoxal by oxidative cleavage [31]. However, all-*trans*-violaxanthin is the isomer typically found in leaves; therefore, *trans*,*trans*-xanthoxal is obtained by its oxidative cleavage. The bioactive geometric isomer can then be obtained by photoisomerization [31], since photochemical activation produces a transient excited state that loses the double-bond character and therefore allows rotation around the bond [57]. The double bond can then re-form upon return to the ground state. As the reaction is photoreversible, a mixture of the geometric isomers is produced that tends to an equilibrium or photostationary state, wherein the *cis*,*trans* isomer (which has a Dreiding energy about 1 kJ/mol higher than the *trans*,*trans* isomer) reaches its maximum equilibrium proportion [57]. Preliminary experiments showed that a maximum proportion of the peak area of *cis*,*trans*-xanthoxal of slightly more than half (about 3/5) that of *trans*,*trans*-xanthoxal could be obtained, in agreement with previous observations [32]. As a *cis* isomer has a slightly smaller peak absorbance than a *trans* isomer [38], it is estimated that a maximum proportion of *cis*,*trans*-xanthoxal of about 40% (of the total xanthoxal) can be obtained by photoisomerization of *trans*,*trans*-xanthoxal, less than originally inferred by Taylor and Burden [31].

For photoisomerization, *trans*,*trans*-xanthoxal was dissolved with 3 mL ACN in a 20-mL glass vial (to reduce UV absorption) and put under blacklight (light source: Philips TL Mini Blacklight Blue TL 6W BLB 1FM, emission at 350–400 nm) for 1–1.5 h (at a distance of about 2 cm from the lamp). Some isomerization at the second double bond could occur during the process, especially if irradiation was too intense (Figure 2B). The reaction time was chosen as the time required for the area of the *cis*,*trans*-xanthoxal peak to become at least half that of the *trans*,*trans*-xanthoxal in reversed-phase HPLC, but before noticeable isomerization at the second double bond occurred (<4% of the total xanthoxal). Thereafter, the sample was diluted with water to 30% ACN, and partitioned to diethyl ether three times. It was finally transferred into a 50-mL round-bottom flask and dried with the rotary evaporator.

3.2.7. Final Purification of Xanthoxal with Normal-Phase SPE

SPE with a 1 g diolic column (Discovery®, Supelco) was carried out (under suction) for the isomer mixture obtained from violaxanthin after photoisomerization as well as for *cis*,*trans*-xanthoxal produced from neoxanthin (without photoisomerization). The xanthoxal sample was dissolved in 2 mL 40:60 ethyl acetate/hexane. The column was deacidified with 5 mL hexane containing 0.5% TEA and conditioned with 10 mL 40:60 ethyl acetate/hexane. After loading the sample, the column was washed with 1 mL 40:60 ethyl acetate/hexane. Xanthoxal was then eluted with 12 mL 40:60 ethyl acetate/hexane: six fractions, 2 mL each, were collected in glass vials. Any residues of butylated hydroxytoluene (coming from diethyl ether, wherein it is commonly present as a stabilizer) and carotenoid fragments were removed with this step. Purity was tested in normal-phase HPLC with an isocratic 70:30 ethyl acetate/hexane flow (as described in the next section). The xanthoxal fractions were united and dried under N_2 flow; the amount of xanthoxal was calculated by the difference compared to the weight of the empty vial, and the sample was stored at +5 °C. For long storage, xanthoxal was kept at −20 °C. On average, about 0.5–2 mg of total

xanthoxal was obtained per kg of fresh maize leaves; this means about 0.2–0.8 mg *cis*,*trans*-xanthoxal was produced (after photoisomerization).

3.3. Chemical Analyses

3.3.1. HPLC Analyses

For the determination of xanthophylls and other carotenoids, normal-phase HPLC was used [58] with a Beckman-System Gold chromatograph (Beckman Instrument Inc., Brea, CA, USA). Twenty µL of each sample (diluted 1:10 with 80:20 hexane/ethyl acetate) was injected and eluted through a 250 mm × 4 mm 5 µm Lichrospher Si60 column (Merck KgaA, Darmstadt, Germany) with a guard column of the same stationary phase. The mobile phase used was a gradient of solvent A (hexane containing 0.05% TEA) and solvent B (ethyl acetate containing 0.05% TEA) with a flow rate of 1 mL/min. The following steps were used: 20% B for 1 min, from 20% to 70% B over 2 min, to 76% B over 6 min, to 100% B over 1 min, constant 100% B for 4 min, to 20% B over 1 min, 20% B for 3 min (18 min total). Absorbance was measured at 436 nm [59] with a photodiode array detector. The different carotenoids (Supplementary Figure S1) were identified based on their spectroscopic characteristics [37,60].

When epoxydic xanthophylls were dissolved in ACN, reversed-phase HPLC was executed with an Agilent 1200 chromatograph (Agilent Technologies, Waldbronn, Germany). Ten µL was loaded with an auto injector and eluted through a 150 × 4.5 mm 5 µm Zorbax Eclipse XDB-C18 analytical column (Agilent Technologies, Waldbronn, Germany) with a guard column. Isocratic elution was performed with 99.8% ACN containing 0.05% TEA and 0.2% aqueous solution of 3% formic acid for 8 min (1mL/min, 25 °C). Absorbance was measured at 450 nm and 285 nm.

To properly distinguish xanthoxal isomers, reversed-phase HPLC was carried out with the Agilent 1200 system, using isocratic elution (1 mL/min, 25 °C) with 40% ACN containing 0.02% TEA. Absorbance was measured at 285 nm for 5 min.

To assess xanthoxal purity after the final SPE, normal-phase HPLC was used with the Beckman-System Gold system. Twenty µL of each sample (diluted twenty times with 70:30 ethyl acetate/hexane) was injected. Isocratic elution (1 mL/min) with 70:30 ethyl acetate/hexane (containing 0.05% TEA) was followed at 280 nm for 7 min. The retention time for the largely overlapping *trans*,*trans*-xanthoxal and *cis*,*trans*-xanthoxal isomers was 4.1 min.

3.3.2. Mass Spectrometry

Mass Spectrometry (MS) analysis was carried out on a mixture of the two geometric isomers obtained from violaxanthin (after photoisomerization) with a Triple-Stage Quadrupole mass spectrometer with an electrospray ionization (ESI^+) source (TSQ Quantum, Thermo Scientific, San Jose, CA, USA). A Surveyor HPLC (shortly, LC) device with a 125 mm × 4 mm × 5 µm C18 column was connected to the spectrometer for LC-(PDA)-ESI-MS and tandem mass spectrometry (MS/MS). 0.1% formic acid in water and ACN were used as solvent A and solvent B, respectively. Elution consisted of a gradient from 5% B to 95% B over 25 min. Absorbance was followed (for 28 min) in the 200–400 nm range with a channel at 285 nm. For LC-ESI-MS, "full mass" signals (every 100 msec) in the 200–400 m/z range were initially analysed to ascertain the absence of other noticeable masses, and the range was then restricted to 220–260 m/z. The only two strong signals observed, namely, the molecular peak at 251 m/z $[M+H]^+$ and its dehydrated form with 233 m/z (Figure 3), were then fragmented in MS/MS. In LC-ESI-MS/MS, the most abundant peak at each microscansion is fragmented with a fixed collision energy (default 30 eV); for xanthoxal, this resulted in a complex fragmentation pattern (Supplementary Figure S3). Hence, direct infusion ESI-MS/MS was performed (with xanthoxal dissolved in methanol), and the collision energy was modulated to a lower level such that the molecular peak did not completely disappear (Supplementary Figure S4).

3.4. Chemical Editor

MarvinSketch and MarvinView (version 19.21.0, 2019; ChemAxon, http://www.chemaxon.com; last accessed on 19 November 2019) were used for drawing, displaying, and characterizing the chemical structures and their 3D conformational isomerism, including the conformer Dreiding energy. The latter represents the relative potential energy of the 3D structure (conformation) of a molecule calculated by using the Dreiding force field after automatic optimization of the molecular structure. The Dreiding energy of the lowest-energy (more stable) conformer was used as an aid to choose the putative structure of the main positively charged fragments, based on their stability, among several potential candidate structures inferred from the mass spectra.

3.5. Seed Materials and Experimental Setup

A straw-hulled red rice genotype originally found in a paddy close to Vercelli (located in a rice-growing area of the Po Valley, Italy), and previously used for other studies [14,16,48,61], was grown in a greenhouse at Fiorenzuola d'Arda (Italy). The seed grains (botanically, the rice dispersal units are spikelets) were harvested when showing shattering capability and dried for 1 d at 35 °C [48]. Dormant red rice spikelets (germination $\leq$ 3% in water) were stored at −15 °C till use [16]. Naked (dehulled) caryopses were prepared by manually dehulling the spikelets prior to the start of the experimental run [16,48]. Although the naked rice grain is botanically a caryopsis, for the sake of simplicity it is referred to as a "seed", in a broad sense, throughout this paper.

Dehulled dormant red rice caryopses produce superoxide for about two days following imbibition [62], and such reactive oxygen species can easily degrade xanthoxal, since it reacts with conjugated dienes [63] (p. 72) so that carbonyl carotenoids, even short-chain ones, easily take up electron pairs [64]. For that reason, and also because of the quick reactivity of the aldehyde group with peroxyl radicals [65], the seeds were pre-imbibed at 30 °C for 2–10 days in plastic Petri dishes (90 mm diameter; VWR International, Milano, Ialy) on two filter paper discs (90 mm diameter; Whatman grade 1, GE Healthcare Life Sciences, Little Chalfont, UK), with 5 mL of water, before testing. Any seed that germinated during pre-imbibition was excluded from the subsequent trials. All the seeds used in a given experimental run were pre-imbibed for the same period of time. The effect of chemicals was then tested by transferring the seeds to 100 mL Erlenmeyer flasks (capped with aluminium foil), enclosed in a humidity box at 30 °C. The seeds were placed on a Whatman 3 MM (GE Healthcare Life Sciences, Little Chalfont, UK) paper disc (4 cm diameter, cut out by hand) with 2 mL of the incubation solution [14]. For each treatment, two to six (typically three) replicate flasks, with 12 caryopses each, were used. All incubation solutions were buffered at pH 4.8 (the pK_a of ABA is 4.75 [40]) with 20 mM BTCA [14]. Acidic conditions enhance ABA effectiveness [14,40] and reduce the production of superoxide by seeds [62]. In the control (dormant seeds without bioactive chemicals), the seeds were incubated in the buffer solution. Treatments with bioactive chemicals also included: 10 µM fluridone, 10 µM fluridone + 10 µM (±)-ABA [14], or 10 µM fluridone + 5 µM *cis*,*trans*-xanthoxal (applied as a mixture of isomers from violaxanthin). The concentrations of fluridone and ABA were the same as used by Gianinetti and Vernieri [14]. Immediately prior to adding fluridone, the diluted buffer solution and the fluridone stock were pre-warmed at about 37 °C to improve the dissolution of fluridone in the aqueous solution. The concentration of *cis*,*trans*-xanthoxal was fixed at 5 µM for optimal comparison: because racemic (±)-ABA is a mixture of S(+) and R(−) forms in approximately equal amounts [39], whereas the naturally occurring form is (S)-*cis*-ABA, also known as (+)-*cis*,*trans*-abscisic acid, the biologically effective xanthoxal isomer, (S)-*cis*,*trans*-xanthoxal (the S structure is the natural structure of ABA precursors), was applied at the same expected concentration as the biologically effective ABA isomer, that is, half the concentration of (±)-ABA. The mixture of isomers produced from violaxanthin was used in the xanthoxal test, and the concentration of *cis*,*trans*-xanthoxal was kept at 5 µM. As very small amounts of xanthoxal were commonly handled, the concentration of *cis*,*trans*-xanthoxal in the incubation solution was adjusted to

the desired concentration (5 µM) on the basis of the corresponding peak area obtained from reversed-phase HPLC. Based on a large sample preparation, it was estimated that, with the described method and using an injected volume of 3 µL, one peak unit area corresponded to a *trans*,*trans*-xanthoxal concentration of about 62 µg/L. Although for *cis*,*trans*-xanthoxal this value ought to be slightly higher, the proportion of the *cis*,*trans*-xanthoxal isomer in the isomer mixture produced from violaxanthin was directly calculated from the area of the HPLC peak, without considering differences in absorbance among isomers. The caryopses were transferred to new flasks with fresh incubation solutions three times a week (on Monday, Wednesday, and Friday). The incubation solutions containing the bioactive chemicals were prepared the day prior to first using them, in amounts enough for one week; they were then stored at +5 °C. Preliminary HPLC checks showed no degradation of the chemicals in the stored aqueous solutions over this time (the solution was quite stable even for several weeks).

Two stages of germination were recorded (at every change of flask): (i) pericarp splitting, the first visible sign of germination in red rice [14], which in cereals is more precisely defined as the rupture of the caryopsis coat [48] and is more generally known as the rupture of the seed testa [17]; and (ii) the first growth stage (S1 [66]), recorded when rootlets or coleoptiles were $\geq$1 mm (minimal visible seedling growth). Stage S1 includes some early seedling growth that makes germination easier to see [67]. Pericarp splitting was determined, with the aid of a magnifier, as the opening of the red caryopsis coat covering the swelling embryo axis into two lips, disclosing the underlying tissues. Seedlings attaining growth stage S1 were always discharged after recording. At the end of each test, non-germinated caryopses were transferred to Petri dishes with two discs of filter paper and 4 mL of water to assess their viability. In fact, the dormancy-breaking effect of fluridone persists well after removal of the exogenous supply, whereas the germination-delaying effect of 10 µM ABA does not, so that viable seeds quickly germinate when the incubation solution is replaced with water [14]. Xanthoxal, which is metabolized to ABA, also loses its effectiveness when no longer provided exogenously. Caryopses that did not attain growth stage S1 in one week of incubation at 30 °C after being transferred to water were considered not viable. The difference between observed percentages of growth in stage S1 and germination was used as an indicator of the delay of seedling growth after germination was attained, i.e., as an indirect measure of the apparent delay of germination. The rationale for this indicator is that if seedling growth is quick, at the time of recording, only a few seeds are observed at the pericarp splitting stage before seedling growth is apparent (as the time between the two stages is very short). As the time between the two stages increases, a higher proportion of seeds is expected to be detected at the pericarp splitting stage before they display seedling growth.

3.6. Statistical Analysis

Statistical analysis of the germination data was performed with the GLIMMIX procedure of the SAS® 9.4 software (SAS® OnDemand for Academics; SAS Institute Inc., Cary, NC, USA) according to a conditional generalized linear mixed model using the probit link function and Laplace approximation of maximum likelihood [68]. The treatment effect was modelled through time as a spline; this was because of the multiple observation times, which differed across experimental runs (the experiment was, in fact, split into many incomplete experimental runs, each typically including two treatments, and each treatment was repeated over three to six experimental runs), and also depended on the day of the week the individual experimental run started. The interaction between treatment and experimental run was modelled as a random factor, and the Petri dish effect was modelled as a random factor with first-order autoregressive covariance structure [68]. Additional information about the statistical analysis, including the SAS code, is given in Appendix A.

4. Conclusions

In red rice seeds whose dormancy is broken by fluridone, exogenously applied xanthoxal is more effective at inhibiting germination than exogenous ABA, but it is ineffective at further delaying early seedling growth once germination (pericarp splitting) is achieved. It remains to be established which of three suggested hypotheses explains this result. The first possibility is that the former effect is a consequence of xanthoxal being a non-ionic compound whilst ABA is a dissociable acid, such that exogenous xanthoxal enters the cells easier than ABA; however, this hypothesis requires some mechanism that prevents the achievement of a corresponding equilibrium between symplastic and apoplastic ABA when either xanthoxal or ABA is exogenously provided. The second possibility is that xanthoxal carries out a competitive inhibition of ABA action in the apoplast, thus suppressing the capability of ABA to delay seedling growth. The final possibility is that xanthoxal plays a specific role in dormancy, that is, it specifically blocks germination rather than seedling growth; however, like for the first possibility, a further mechanism must be invoked to explain the inhibition of seedling growth by exogenous ABA only. Thus, both the first and the third hypotheses imply the existence of a physiological restraint on ABA export/import, at least when ABA reaches some biologically meaningful threshold. In any case, the contrasting effects of exogenous xanthoxal on pericarp splitting and early seedling growth, compared to exogenous ABA, indicate that different receptors are involved in these two processes. As a tentative explanation, it is here proposed that symplastic receptors are involved in the regulation of seed germination, whereas apoplastic ABA receptors control early seedling growth. It is certain that extracellular ABA was required to inhibit early seedling growth.

Supplementary Materials: The following supporting information can be downloaded at: https://www.mdpi.com/article/10.3390/plants11081023/s1, Figure S1: HPLC analysis of the raw extract; Figure S2: 3D chromatogram; Figure S3: LC-ESI-MS/MS fragmentation analysis; Figure S4: Direct infusion ESI-MS/MS fragmentation analysis; Figure S5: Aspect of the embryo collar and development of rhizoids.

Funding: This research received no external funding.

Institutional Review Board Statement: Not applicable.

Informed Consent Statement: Not applicable.

Data Availability Statement: The data presented in this study are openly available in Zenodo at https://doi.org/10.5281/zenodo.6424237.

Acknowledgments: I thank Alberto Sala (Sipcam S.p.A.) for carrying out LC-(PDA)-ESI-MS analysis and Renzo Alberici for assistance with the photography.

Conflicts of Interest: The author declares no conflict of interest.

Appendix A

Statistical Details and Notes

The experiment was split into many experimental runs (that is, trials or repetitions of the treatments) carried out from the end of 2019 to the beginning of 2022. Experimental runs were incomplete: only a pair of treatments, in different combinations across experimental runs, were typically included in each run. On the one hand, this design has some advantages: it improves the control of random effects and minimizes the effects of uncontrolled variables as well as the impact of errors made in any one experimental run by averaging together the results of each treatment across multiple treatment repeats (independent repetitions of the trial for a given treatment). For example, a new xanthoxal stock was independently produced for each experimental run that included seeds treated with this chemical. In addition, due to the COVID-19 pandemic, there was a high risk of having to prematurely stop the experiment at any time because missing a change of the incubation solutions on a planned date was considered to invalidate the subsequent

observations. This was problematic, especially for the treatment with xanthoxal, which then had to be produced again for a new treatment repeat. In fact, some experimental runs were prematurely truncated. When they demonstrated a clear trend (i.e., they lasted at least two weeks), these datasets were nonetheless retained. On the other hand, although the aggregate results show very clear trends (see Figure 4), this experimental design is intractable with classical statistical analysis. In fact, it is equipollent to an incomplete block design (where the experimental run can be considered a block effect) in which each block (experimental run) received only some of the treatments to be compared. Typically, two different treatments were run together, variously assorted across experimental runs, but not in all possible combinations, so that the design is also unbalanced, because not all possible pairs of treatments occurred. Moreover, the observation times differed between experimental runs. The aggregate data, however, are suited to curve fitting, because of their smooth trends. In this respect, splines (continuous curvilinear interpolations based on piecewise polynomials that allow empirical estimations of the mean functions) provide a versatile tool for managing these kinds of data and making them suitable for statistical analysis with generalized linear mixed models (GzLMMs) [68]. Interpolation also addresses the problem that the timepoints are unequally spaced and differ across experimental runs. The following SAS code (see SAS/STAT® 15.1 User's Guide, version 2021.2.5; SAS Institute Inc., Cary, NC, US), based on the conditional model with continuous time and integral approximation described in Annex S-IV of [68], was therefore implemented to analyse the data:

```
/* conditional model with continuous time */
proc GLIMMIX method = Laplace;
effect spltime = spline(day);
class rep exp trt;
model VAR/n = trt trt * spltime/link = probit;
random trt * exp;
random rep(trt * exp)/type = AR(1);
lsmeans trt/at day = 10 adjust = sidak stepdown ilink;
lsmeans trt/at day = 20 adjust = sidak stepdown ilink;
lsmestimate trt 'D vs. D + F + A' 1 0 −1 0 0,
'D vs. D + F + X' 1 0 0 −1 0,
'D + F + A vs. D + F + X' 0 0 1 −1 0/
at day = 20 adjust = sidak stepdown elsm;
run;
```

where "VAR" stands for the actual dependent variable used in each statistical analysis, namely: germination (pericarp splitting), early seedling growth (growth stage S1), and their difference. In addition, 'rep' is the replicate Petri dish within each treatment repeat, 'exp' is the experimental run, and 'trt' is the treatment. Response variables were corrected for seeds that appeared not viable (rot) during the experiment (by adjusting 'n', the number of tested seeds), but were not further corrected for viability as assessed, ex post, with the viability test, because it was close to 100% in every treatment.

Although data on the germination lag time (for pre-imbibed seeds, this is the initial time during which no germination occurs in any tested condition) must commonly be removed from the dataset for statistical analysis based on GzLMMs, nevertheless, since means with null values cannot be modelled on the linear (probit) scale [68], the initial lag time was practically zeroed in the present case using pre-imbibed seeds. Not even data for time zero (which were all 0s, since only non-germinating seeds were used for this experiment) had to be removed because if only very few timepoints correspond to the limit values, splines can still be modelled on the probit scale. This is because they tend to slightly move away from the limit values of the data scale, thereby attenuating extreme means. Correspondingly, splines, similar to other kinds of empirical curve-fitting, require that once the germination time-course for a given treatment, and for the whole treatment across all the experimental runs, reaches its theoretical maximum (i.e., 1, or 100% in percent terms), no further records are taken. This is because they would stay the same ad infinitum, thereby creating a plateau that is unmanageable on the linked scale. This means that data of 100% for individual replicates, as well as for treatment repeats, are retained till all reach

100%. Afterwards, for each tested condition, any output statistical inference is meaningless. Moreover, because the errors of the estimates are hugely inflated when a spline approaches limit values (0s and 1s proportions on the data scale), statistical tests should be avoided at timepoints at which even one spline is in this critical condition.

In this respect, it is noted that, when true likelihood is used in GzLMMs, only means are modelled on the linked scale (where 0s and 1s cannot be transposed), whereas the single observations are modelled on the data scale, where 0 s and 1 s (0% and 100%, respectively) are not a problem. Thus, Laplace approximation to maximum-likelihood was used to prevent modelling individual data on the linked scale by pseudo-likelihood (which, instead, models all the data on the linked scale), since, as stated, some 0s and 1s were present. The use of marginal and quasi-marginal models [68], was therefore prevented. This GzLMM approach was useful for handling datasets with several, though not too many, limit data.

A conditional model is particularly well adapted when the difference between proportions occurring at two different stages in each Petri dish (cluster of seeds) is considered: as the proportion of seeds at each stage is recorded over the whole dish, the proportion of seeds that attain one stage but not the other is averaged across the dish too, and it does not refer to individual seeds, since seeds are not tracked as individual entities through subsequent observations. A conditional model, indeed, provides a conditional mean that represents the expectation of the sample proportion of the mean dish, not of the marginal distribution of the seeds.

The model includes two fixed effects: 'trt' and 'trt * spltime'. They correspond to the intercept and the trend of each treatment, respectively [68] (Annex S-IV). In fact, the Tests of Fixed Effects (Tables A1–A3) indicate a non-significant effect for 'trt' (as expected, because the intercept was always 0 by design, since only non-germinating seeds were used for the experiment) and a highly significant effect for 'trt * spltime', which means that what the treatments caused in this experiment was not a vertical shift of an overall curvilinear trend (assessed at time = 0, since 'trt' is modelled in terms of a separate intercept for each treatment when a spline effect is present), but rather a change of its shape. As the shape of the germination time-course was clearly different among treatments, this diversity has been modelled in terms of the interaction between treatment and spline, i.e., 'trt * spltime'; whereas a simple 'spltime' effect would have modelled all the time-courses with the same curve, which was not the case here. However, this could be added as a general trend, but with no benefit to the model, since it would still need to be further modified for each treatment level by the 'trt * spltime' effect.

Table A1. Test of Fixed Effects for germination.

Type III Tests of Fixed Effects				
Effect	**Num DF**	**Den DF**	**F Value**	**Pr > F**
trt	4	726	0.72	0.5802
spltime*trt	26	726	49.47	<0.0001

Table A2. Test of Fixed Effects for early seedling growth.

Type III Tests of Fixed Effects				
Effect	**Num DF**	**Den DF**	**F Value**	**Pr > F**
trt	4	726	0.37	0.8305
spltime*trt	26	726	27.63	<0.0001

Table A3. Test of Fixed Effects for growth delay.

Type III Tests of Fixed Effects				
Effect	**Num DF**	**Den DF**	**F Value**	**Pr > F**
trt	4	726	0.11	0.9796
spltime*trt	23	726	18.61	<0.0001

As the 'trt' effect was null by design (at least, in a continuous model where it is specifically modelled as intercept), it could have been omitted from the model. However, it provides a check for the model fitting, and it is also needed to estimate the means and test them at the requested timepoints, as the 'lsmeans' and 'lsmestimate' statements require that the effect for which the comparisons are made be in the model.

Two random effects were included in the model: the interaction between treatment and experimental run ('trt * exp') and the effect of the individual Petri dish ('rep(trt * exp)'), the latter being explicitly nested within each experimental run and treatment combination because the replicates had the same labels (namely, 1, 2, 3) across the different treatments and experimental runs. The interaction between treatment and experimental run ('trt * exp') corresponds to the treatment repeat; given that the fixed 'trt' is, contingently to the presence of a spline effect, demoted from determining the slope of the linear response function to specifying a distinct intercept for each treatment (albeit all null by design, in the present experiment), differences among the repeats are modelled as random intercepts as well (that is, they represent random up-and-down fluctuations of the 'trt * spltime' trends). A random effect for the experimental run ('exp') was not included, since the 'exp' effect would be modelled as a random intercept for each experimental run; therefore, not only it would be unnecessary (as with the 'spltime' effect in the specification of the fixed factors), but it would also largely overlap with the 'trt * exp' effect because of the strongly incomplete design (i.e., only two out of five treatments were included in each experimental run). As this caused a few problems for the estimation of the model, and the AICC fit statistic (useful for evaluating this kind of model [68]) showed a slightly worse fit if this effect was included, it was excluded from the model.

A first-order autoregressive covariance structure ('type = AR(1)') was used to account for the non-independence of the observations made on the same Petri dish over time [68].

Tests of the covariance parameters (with the 'covtest' statement; not shown), showed that the treatment repeat random effect ('trt * exp'), unlike the Petri dish ('rep') effect (specified, as said, as 'rep(trt * exp)'), was non-significant; that is, the variability among experimental runs was negligible. A non-significant effect was also observed for the first-order autoregressive covariance structure ('type = AR(1)'), probably due to the fast germinating treatments (D + F and D + F + tX), wherein subsequent observations differ a lot. Both the treatment repeat random effect and the AR(1) covariance structure were nonetheless retained because they represent characteristic features of the design.

Two timepoints were tested for the differences among treatments: 10 d and 20 d. Although the key differences among the treatments are evident, these tests provide statistical support for the present findings. The two timepoints were chosen so that no spline was too close to limit values (0% and 100%; one exception is discussed below), but the most interesting differences among the treatments could still be evidenced. The 'ilink' option of the 'lsmeans' statements requests that the estimated means and their standard errors are also reported on the data scale (i.e., the inverse linked scale).

An adjustment of probability for multiplicity of comparisons was conducted at each timepoint for the number of pairwise comparisons among treatments based on the Sidak test ('adjust = sidak'), further adjusted in a step-down fashion (Holm's procedure) to increase the power of multiple comparisons ('stepdown'). No correction for the number of timepoints at which the comparisons were made (two) was adopted because, although it would be compelling in any other case, in longitudinal germination studies an adjustment of probability across timepoints is usually not necessary when germination time-courses are

modelled as a continuous function of time (since using a smooth fitted function for statistical tests, rather than the discrete original data, reduces the risk of stochastic fluctuations at individual timepoints of the germination progress curve) and one just needs to test neat trends for significant differences [68].

An 'lsmestimate' statement was additionally used to compute the adjusted probabilities for comparisons at day 20, since only three treatments had estimable least-squares means at that timepoint. Because of the inestimability of two means (namely, those of D + F and D + F + tX), step-down adjusted *P*-values could not be computed at that timepoint. While the 'lsmeans' statement automatically provides the whole set of pairwise comparisons when an 'adjust=' option is present, the 'lsmestimate' statement allows testing specific hypotheses among the least-squares means; inestimable means can thus be excluded. The comparisons between treatment means estimable at day 20 were therefore individually specified, and the 'elsm' option was used to check that they were correctly contrasted.

Finally, as most treatments (D + F + A excluded) had many null values for the difference between early seedling growth and germination percentages (the variable measuring delay of seedling growth), the splines were too close to the limit value (0%) to produce accurate estimates of the errors of the least-squares means and, therefore, reliable statistical inference about the differences between means. Thus, a corresponding mixed model using angular (arcsine) transformed data was used [68] to assess the statistical differences between treatments for this response variable.

References

1. Bewley, J.D.; Bradford, K.J.; Hilhorst, H.W.M.; Nonogaki, H. *Seeds: Physiology of Development, Germination and Dormancy*, 3rd ed.; Springer: New York, NY, USA, 2013; ISBN 978-1-4614-4692-7.
2. Ziska, L.H.; Gealy, D.R.; Burgos, N.; Caicedo, A.L.; Gressel, J.; Lawton-Rauh, A.L.; Avila, L.A.; Theisen, G.; Norsworthy, J.; Ferrero, A.; et al. Weedy (Red) Rice: An Emerging Constraint to Global Rice Production. *Adv. Agron.* **2015**, *129*, 181–228. [CrossRef]
3. Cohn, M.A. Chemical Mechanisms of Breaking Seed Dormancy. *Seed Sci. Res.* **1996**, *6*, 95–99. [CrossRef]
4. Chao, W.S.; Horvath, D.P.; Anderson, J.V.; Foley, M.E. Potential Model Weeds to Study Genomics, Ecology, and Physiology in the 21st Century. *Weed Sci.* **2005**, *53*, 929–937. [CrossRef]
5. Liu, X.; Hou, X. Antagonistic Regulation of ABA and GA in Metabolism and Signaling Pathways. *Front. Plant Sci.* **2018**, *9*, 251. [CrossRef] [PubMed]
6. Chen, K.; Li, G.; Bressan, R.A.; Song, C.; Zhu, J.; Zhao, Y. Abscisic Acid Dynamics, Signaling, and Functions in Plants. *J. Integr. Plant Biol.* **2020**, *62*, 25–54. [CrossRef] [PubMed]
7. Schopfer, P.; Bajracharya, D.; Plachy, C. Control of Seed Germination by Abscisic Acid: I. Time Course of Action in *Sinapis alba* L. *Plant Physiol.* **1979**, *64*, 822–827. [CrossRef] [PubMed]
8. Lopez-Molina, L.; Mongrand, S.; Chua, N.-H. A Postgermination Developmental Arrest Checkpoint Is Mediated by Abscisic Acid and Requires the ABI5 Transcription Factor in *Arabidopsis*. *Proc. Natl. Acad. Sci. USA* **2001**, *98*, 4782–4787. [CrossRef]
9. Koornneef, M.; Jorna, M.L.; Brinkhorst-van der Swan, D.L.C.; Karssen, C.M. The Isolation of Abscisic Acid (ABA) Deficient Mutants by Selection of Induced Revertants in Non-Germinating Gibberellin Sensitive Lines of *Arabidopsis thaliana* (L.) Heynh. *Theor. Appl. Genet.* **1982**, *61*, 385–393. [CrossRef]
10. Frey, A.; Effroy, D.; Lefebvre, V.; Seo, M.; Perreau, F.; Berger, A.; Sechet, J.; To, A.; North, H.M.; Marion-Poll, A. Epoxycarotenoid Cleavage by NCED5 Fine-Tunes ABA Accumulation and Affects Seed Dormancy and Drought Tolerance with Other NCED Family Members. *Plant J.* **2012**, *70*, 501–512. [CrossRef]
11. Groot, S.P.C.; Karssen, C.M. Dormancy and Germination of Abscisic Acid-Deficient Tomato Seeds: Studies with the *Sitiens* Mutant. *Plant Physiol.* **1992**, *99*, 952–958. [CrossRef]
12. Marin, E.; Nussaume, L.; Quesada, A.; Gonneau, M.; Sotta, B.; Hugueney, P.; Frey, A.; Marion-Poll, A. Molecular Identification of Zeaxanthin Epoxidase of *Nicotiana plumbaginifolia*, a Gene Involved in Abscisic Acid Biosynthesis and Corresponding to the ABA Locus of *Arabidopsis thaliana*. *EMBO J.* **1996**, *15*, 2331–2342. [CrossRef] [PubMed]
13. Wang, M.; Heimovaara-Dijkstra, S.; Van Duijn, B. Modulation of Germination of Embryos Isolated from Dormant and Nondormant Barley Grains by Manipulation of Endogenous Abscisic Acid. *Planta* **1995**, *195*, 586–592. [CrossRef]
14. Gianinetti, A.; Vernieri, P. On the Role of Abscisic Acid in Seed Dormancy of Red Rice. *J. Exp. Bot.* **2007**, *58*, 3449–3462. [CrossRef] [PubMed]
15. Goggin, D.E.; Steadman, K.J.; Emery, R.J.N.; Farrow, S.C.; Benech-Arnold, R.L.; Powles, S.B. ABA Inhibits Germination but Not Dormancy Release in Mature Imbibed Seeds of *Lolium rigidum* Gaud. *J. Exp. Bot.* **2009**, *60*, 3387–3396. [CrossRef] [PubMed]
16. Gianinetti, A.; Finocchiaro, F.; Bagnaresi, P.; Zechini, A.; Faccioli, P.; Cattivelli, L.; Valè, G.; Biselli, C. Seed Dormancy Involves a Transcriptional Program That Supports Early Plastid Functionality during Imbibition. *Plants* **2018**, *7*, 35. [CrossRef]

17. Weitbrecht, K.; Müller, K.; Leubner-Metzger, G. First off the Mark: Early Seed Germination. *J. Exp. Bot.* **2011**, *62*, 3289–3309. [CrossRef]
18. Millar, A.A.; Jacobsen, J.V.; Ross, J.J.; Helliwell, C.A.; Poole, A.T.; Scofield, G.; Reid, J.B.; Gubler, F. Seed Dormancy and ABA Metabolism in Arabidopsis and Barley: The Role of ABA 8′-Hydroxylase. *Plant J.* **2006**, *45*, 942–954. [CrossRef]
19. Liu, A.; Gao, F.; Kanno, Y.; Jordan, M.C.; Kamiya, Y.; Seo, M.; Ayele, B.T. Regulation of Wheat Seed Dormancy by After-Ripening Is Mediated by Specific Transcriptional Switches That Induce Changes in Seed Hormone Metabolism and Signaling. *PLoS ONE* **2013**, *8*, e56570. [CrossRef]
20. Carrera, E.; Holman, T.; Medhurst, A.; Dietrich, D.; Footitt, S.; Theodoulou, F.L.; Holdsworth, M.J. Seed After-Ripening Is a Discrete Developmental Pathway Associated with Specific Gene Networks in Arabidopsis. *Plant J.* **2008**, *53*, 214–224. [CrossRef]
21. Chibani, K.; Ali-Rachedi, S.; Job, C.; Job, D.; Jullien, M.; Grappin, P. Proteomic Analysis of Seed Dormancy in Arabidopsis. *Plant Physiol.* **2006**, *142*, 1493–1510. [CrossRef]
22. Matusova, R.; Rani, K.; Verstappen, F.W.A.; Franssen, M.C.R.; Beale, M.H.; Bouwmeester, H.J. The Strigolactone Germination Stimulants of the Plant-Parasitic *Striga* and *Orobanche* spp. Are Derived from the Carotenoid Pathway. *Plant Physiol.* **2005**, *139*, 920–934. [CrossRef] [PubMed]
23. Ali-Rachedi, S.; Bouinot, D.; Wagner, M.-H.; Bonnet, M.; Sotta, B.; Grappin, P.; Jullien, M. Changes in Endogenous Abscisic Acid Levels during Dormancy Release and Maintenance of Mature Seeds: Studies with the Cape Verde Islands Ecotype, the Dormant Model of *Arabidopsis thaliana*. *Planta* **2004**, *219*, 479–488. [CrossRef] [PubMed]
24. Leymarie, J.; Benech-Arnold, R.L.; Farrant, J.M.; Corbineau, F. Thermodormancy and ABA Metabolism in Barley Grains. *Plant Signal. Behav.* **2009**, *4*, 205–207. [CrossRef] [PubMed]
25. Alvarado, V.; Bradford, K.J. Hydrothermal Time Analysis of Seed Dormancy in True (Botanical) Potato Seeds. *Seed Sci. Res.* **2005**, *15*, 77–88. [CrossRef]
26. Grappin, P.; Bouinot, D.; Sotta, B.; Miginiac, E.; Jullien, M. Control of Seed Dormancy in *Nicotiana plumbaginifolia*: Post-Imbibition Abscisic Acid Synthesis Imposes Dormancy Maintenance. *Planta* **2000**, *210*, 279–285. [CrossRef] [PubMed]
27. Chae, S.H.; Yoneyama, K.; Takeuchi, Y.; Joel, D.M. Fluridone and Norflurazon, Carotenoid-Biosynthesis Inhibitors, Promote Seed Conditioning and Germination of the Holoparasite *Orobanche minor*. *Physiol. Plant* **2004**, *120*, 328–337. [CrossRef]
28. Awan, S.Z.; Chandler, J.O.; Harrison, P.J.; Sergeant, M.J.; Bugg, T.D.H.; Thompson, A.J. Promotion of Germination Using Hydroxamic Acid Inhibitors of 9-Cis-Epoxycarotenoid Dioxygenase. *Front. Plant Sci.* **2017**, *8*, 357. [CrossRef]
29. Erb, M.; Glauser, G. Family Business: Multiple Members of Major Phytohormone Classes Orchestrate Plant Stress Responses. *Chem. Eur. J.* **2010**, *16*, 10280–10289. [CrossRef]
30. Kepka, M.; Benson, C.L.; Gonugunta, V.K.; Nelson, K.M.; Christmann, A.; Grill, E.; Abrams, S.R. Action of Natural Abscisic Acid Precursors and Catabolites on Abscisic Acid Receptor Complexes. *Plant Physiol.* **2011**, *157*, 2108–2119. [CrossRef]
31. Taylor, H.F.; Burden, R.S. Xanthoxin, a Recently Discovered Plant Growth Inhibitor. *Proc. R. Soc. Lond. B Biol. Sci.* **1972**, *180*, 317–346. [CrossRef]
32. Milborrow, B.V.; Burden, R.S.; Taylor, H.F. Xanthoxal: A Revision of the Nomenclature of the ABA Precursor Xanthoxin. *Phytochemistry* **1997**, *44*, 977–978. [CrossRef]
33. Xia, Q.; Ponnaiah, M.; Thanikathansubramanian, K.; Corbineau, F.; Bailly, C.; Nambara, E.; Meimoun, P.; El-Maarouf-Bouteau, H. Re-Localization of Hormone Effectors Is Associated with Dormancy Alleviation by Temperature and after-Ripening in Sunflower Seeds. *Sci. Rep.* **2019**, *9*, 4861. [CrossRef]
34. Laspina, N.V.; Batlla, D.; Benech-Arnold, R.L. Dormancy Cycling Is Accompanied by Changes in ABA Sensitivity in Polygonum Aviculare Seeds. *J. Exp. Bot.* **2020**, *71*, 5924–5934. [CrossRef] [PubMed]
35. Zeevaart, J.A.D. Levels of (+)-Abscisic Acid and Xanthoxin in Spinach under Different Environmental Conditions. *Plant Physiol.* **1974**, *53*, 644–648. [CrossRef] [PubMed]
36. Häckl, K.; Kunz, W. Some Aspects of Green Solvents. *Comptes Rendus Chim.* **2018**, *21*, 572–580. [CrossRef]
37. Parry, A.D.; Babiano, M.J.; Horgan, R. The Role of *Cis*-Carotenoids in Abscisic Acid Biosynthesis. *Planta* **1990**, *182*, 118–128. [CrossRef]
38. Hernandez-Marin, E.; Galano, A.; Martínez, A. *Cis* Carotenoids: Colorful Molecules and Free Radical Quenchers. *J. Phys. Chem. B* **2013**, *117*, 4050–4061. [CrossRef]
39. Li, J.; Wu, Y.; Xie, Q.; Gong, Z. Abscisic Acid. In *Hormone Metabolism and Signaling in Plants*; Li, J., Li, C., Smith, S.M., Eds.; Academic Press: London, UK, 2017; pp. 161–202. ISBN 978-0-12-811562-6.
40. Bruggeman, F.J.; Libbenga, K.R.; Duijn, B. The Diffusive Transport of Gibberellins and Abscisic Acid through the Aleurone Layer of Germinating Barley Grain: A Mathematical Model. *Planta* **2001**, *214*, 89–96. [CrossRef]
41. Boursiac, Y.; Léran, S.; Corratgé-Faillie, C.; Gojon, A.; Krouk, G.; Lacombe, B. ABA Transport and Transporters. *Trends Plant Sci.* **2013**, *18*, 325–333. [CrossRef]
42. Park, J.; Lee, Y.; Martinoia, E.; Geisler, M. Plant Hormone Transporters: What We Know and What We Would like to Know. *BMC Biol.* **2017**, *15*, 93. [CrossRef]
43. Kang, J.; Yim, S.; Choi, H.; Kim, A.; Lee, K.P.; Lopez-Molina, L.; Martinoia, E.; Lee, Y. Abscisic Acid Transporters Cooperate to Control Seed Germination. *Nat. Commun.* **2015**, *6*, 8113. [CrossRef] [PubMed]
44. Kato-Noguchi, H. Allelopathic Substances in *Pueraria thunbergiana*. *Phytochemistry* **2003**, *63*, 577–580. [CrossRef]

45. Kang, J.; Lee, Y.; Martinoia, E. How Can We Interpret the Large Number and Diversity of ABA Transporters? In *Progress in Botany*; Cánovas, F.M., Lüttge, U., Risueño, M.-C., Pretzsch, H., Eds.; Springer International Publishing: Cham, Switzerland, 2020; Volume 82, pp. 233–257. ISBN 978-3-030-68619-2.
46. Todoroki, Y. ABA and Its Derivatives: Chemistry and Physiological Functions. In *Abscisic Acid: Metabolism, Transport and Signaling*; Zhang, D.-P., Ed.; Springer: Dordrecht, The Netherlands, 2014; pp. 1–20. ISBN 978-94-017-9423-7.
47. Parry, A.D.; Neill, S.J.; Horgan, R. Xanthoxin Levels and Metabolism in the Wild-Type and Wilty Mutants of Tomato. *Planta* **1988**, *173*, 397–404. [CrossRef] [PubMed]
48. Gianinetti, A. Anomalous Germination of Dormant Dehulled Red Rice Seeds Provides a New Perspective to Study the Transition from Dormancy to Germination and to Unravel the Role of the Caryopsis Coat in Seed Dormancy. *Seed Sci. Res.* **2016**, *26*, 124–138. [CrossRef]
49. Pawela, A.; Banasiak, J.; Biała, W.; Martinoia, E.; Jasiński, M. Mt ABCG 20 Is an ABA Exporter Influencing Root Morphology and Seed Germination of *Medicago truncatula*. *Plant J.* **2019**, *98*, 511–523. [CrossRef]
50. Srivastava, L.M. *Plant Growth and Development: Hormones and Environment*; Academic Press: Boston, MA, USA, 2002; ISBN 978-0-12-660570-9.
51. Dörffling, K. The Possible Rôle of Xanthoxin in Plant Growth and Development. *Philos. Trans. R. Soc. Lond. B Biol. Sci.* **1978**, *284*, 499–507. [CrossRef]
52. Ruiz-Partida, R.; Rosario, S.M.; Lozano-Juste, J. An Update on Crop ABA Receptors. *Plants* **2021**, *10*, 1087. [CrossRef]
53. Wang, X.-F.; Zhang, D.-P. ABA Signal Perception and ABA Receptors. In *Abscisic Acid: Metabolism, Transport and Signaling*; Zhang, D.-P., Ed.; Springer: Dordrecht, The Netherlands, 2014; pp. 89–116. ISBN 978-94-017-9423-7.
54. Finkelstein, R.R.; Lynch, T.J. Abscisic Acid Inhibition of Radicle Emergence but Not Seedling Growth Is Suppressed by Sugars. *Plant Physiol.* **2000**, *122*, 1179–1186. [CrossRef]
55. Katayama, H.; Miyahara, M. Liquid−liquid Phase Equilibria of (Ethanol or Methanol + Water) Containing Either Dipotassium Hydrogen Phosphate or Sodium Dihydrogen Phosphate. *J. Chem. Eng. Data* **2006**, *51*, 914–918. [CrossRef]
56. Schertz, F.M. The Extraction and Separation of Chlorophyll (A+β) Carotin and Xanthophyll in Fresh Green Leaves, Preliminary to Their Quantitative Determination. *Plant Physiol.* **1928**, *3*, 211–216. [CrossRef]
57. Bochet, C.G. Photochemical Activation of Functional Groups. *Adv. Org. Synth.* **2005**, *1*, 3–23. [CrossRef]
58. Craft, N.E. Chromatographic Techniques for Carotenoid Separation. *Curr. Protoc. Food Anal. Chem.* **2001**, *00*, F2.3.1–F2.3.15. [CrossRef]
59. Schwartz, S.H.; Tan, B.C.; Gage, D.A.; Zeevaart, J.A.D.; McCarty, D.R. Specific Oxidative Cleavage of Carotenoids by VP14 of Maize. *Science* **1997**, *276*, 1872–1874. [CrossRef] [PubMed]
60. Meléndez-Martínez, A.J.; Britton, G.; Vicario, I.M.; Heredia, F.J. Relationship between the Colour and the Chemical Structure of Carotenoid Pigments. *Food Chem.* **2007**, *101*, 1145–1150. [CrossRef]
61. Gianinetti, A.; Cohn, M.A. Seed Dormancy in Red Rice. XII. Population-Based Analysis of Dry-Afterripening with a Hydrotime Model. *Seed Sci. Res.* **2007**, *17*, 253–271. [CrossRef]
62. Ghotbzadeh, S.; Gianinetti, A. A Response of the Imbibed Dormant Red Rice Caryopsis to Biotic Challenges Involves Extracellular PH Increase to Elicit Superoxide Production. *Seed Sci. Res.* **2018**, *28*, 261–271. [CrossRef]
63. Coyle, J.D. *Introduction to Organic Photochemistry*; Wiley: Chichester, UK, 1986; ISBN 978-0-471-90974-3.
64. Zeeshan, M.; Sliwka, H.-R.; Partali, V.; Martínez, A. Electron Uptake by Classical Electron Donators: Astaxanthin and Carotenoid Aldehydes. *Tetrahedron Lett.* **2012**, *53*, 4522–4525. [CrossRef]
65. Denisov, E.T.; Afanas′ev, I.B. *Oxidation and Antioxidants in Organic Chemistry and Biology*; Taylor & Francis: Boca Raton, FL, USA, 2005; ISBN 978-0-8247-5356-6.
66. Counce, P.A.; Keisling, T.C.; Mitchell, A.J. A Uniform, Objective, and Adaptive System for Expressing Rice Development. *Crop. Sci.* **2000**, *40*, 436. [CrossRef]
67. Gianinetti, A.; Laarhoven, L.J.J.; Persijn, S.T.; Harren, F.J.M.; Petruzzelli, L. Ethylene Production Is Associated with Germination but Not Seed Dormancy in Red Rice. *Ann. Bot.* **2007**, *99*, 735–745. [CrossRef]
68. Gianinetti, A. Basic Features of the Analysis of Germination Data with Generalized Linear Mixed Models. *Data* **2020**, *5*, 6. [CrossRef]